Advances in Automotive Engineering, *Vol. 1, No. 1 (2018) 41-59*
DOI: https://doi.org/10.12989/aae.2018.1.1.041

Composite material optimization for heavy duty chassis by finite element analysis

Recep Ufuk* and Murat Ereke

Department of Mechanical Engineering, Istanbul Technical University, Gümüşsuyu No.65, Beyoğlu 34437, Turkey

(Received November 30, 2016, Revised February 11, 2018, Accepted March 12, 2018)

Abstract. In the study, investigation of fiber- reinforced composite materials that can be an alternative to conventional steel was performed by finite element analysis with the help of software. Steel and composite materials have been studied on a four axle truck chassis model. Three-dimensional finite element model was created with software, and then analyzes were performed. The analyses were performed for static and dynamic/fatigue cases. Fatigue cases are formed with the help of design spectra model and fatigue analyses were performed as static analyses with this design spectra. First, analyses were performed for steel and after that optimization analyses were made for the AS4-PEEK carbon fiber composite and Eglass-Epoxy fiber composite materials. Optimization of composite material analyzes include determining the total laminate thickness, thickness of each ply, orientation of each ply and ply stacking sequence. Analyzes were made according to macro mechanical properties of composite, micromechanics case has not been considered. Improvements in weight reduction up to %50 provided at the end of the composite optimization analyzes with satisfying stiffness performance of chassis. Fatigue strength of the composite structure depends on various factors such as, fiber orientation, ply thickness, ply stack sequence, fiber ductility, ductility of the matrix, loading angle. Therefore, the accuracy of theoretical calculations and analyzes should be correlated by testing.

Keywords: laminated composites; optimization; fatigue analysis; finite element analysis; chassis

1. Introduction

The transportation industry plays a key role in the economy. It is obvious that the technical developments to be shown in this area will make many contributions on the economy. The role of heavy vehicles in transportation and other fields is increasing day by day. Improvements in the weight of these vehicles will increase their ability to transport more product, as well as reduce fuel consumption considerably. At the same time, the reduction in weight will also make a positive contribution in reduction of exhaust emissions. Reducing the size and weight of the vehicles also significantly reduces fuel consumption. The US Department of Energy (2013) predicted that a reduction of 35% in vehicle weight will provide fuel savings of 12-20%.

*Corresponding author, E-mail: ufuk@itu.edu.tr

http://www.techno-press.org/?journal=csm&subpage=8 ISSN: 2234-2184 (Print), 2234-2192 (Online)

Heavy-duty vehicle chassis is usually made of steel material, and ladder frame chassis are usually preferred for these vehicles. The chassis constitutes 20-25% of the weight in heavy vehicles. The weight reduction that can be provided in this structure will have positive effects on vehicle performance and usage.

Fiber reinforced composite materials show superior properties compared to metals especially in applications where lightness is required. Composite materials are widely used in wind turbine blades, aircraft and automotive industries. Composite materials are continuously exposed to repeated loads in these components. There is no general form for the behavior of composites under repeated loads. As can be seen from the researches (Campbell 2010, Talreja and Singh 2012, Tsai 1996), each composite structure shows its own fatigue characteristics and these characteristics have to be determined by many tests.

In literature there are some specific studies for vehicles with composite frames. Knouff *et al.* (2006) studied on the design of carrier parts with composite material in Class 7 / Class 8 heavy vehicles. In addition to providing serious results on weight reduction with composite materials in Class 8 tractors, the study has made important proposals on applicability. This study investigated the damage mechanisms of composite materials with progressive damage models by the help of finite element analysis.

In 2003, Daimler Chrysler conducted hybrid frame tests for SUV-type vehicles. The results show that the hybrid frame provides the required strength and durability in terms of vehicle performance criteria. Lavender *et al.* (2006) further improved the frame with computer-assisted analyzes and achieved a weight reduction of 35%. After that, the frame mounted on Dodge Durango vehicle and tests were carried out in vehicle simulators. The hybrid frame successfully sustained the desired design life.

The aim of this study is to examine the applicability of composite materials in the conventional components that are used in the automotive industry. Here, a 4-axle truck chassis model is used with steel and composite materials. AS4-PEEK carbon fiber reinforced composite and Eglass-epoxy glass fiber reinforced composite were used as composite material. In the study Hypermesh and Optistruct packages of Hyperworks software were used. The 3D model of the chassis was modeled with finite elements through this program and then analyzed. The analyses were performed in two groups, static state and dynamic state (fatigue case) by design spectra. The fatigue model was created with the help of a design spectra and the fatigue analysis was performed as a static analysis by this spectrum. After analyzing the steel material firstly, the composite materials in the structure was optimized with software for different composite materials according to stiffness criteria. The optimization of the composite material consists, the total laminate thickness optimization, thickness optimization, fiber orientation and ply stack sequence. For the composite materials in the analyses, macro mechanical properties were considered using classical composite laminate plate theory, and the micro mechanical state was not considered. By this way composite plies can be defined as orthotropic materials and fiber-matrix formation is taken as one material.

At the end of the analyses, both static strength control and fatigue control were carried out. The fatigue life control is done considering the vertical and lateral forces for the steel material. However, for simplicity, optimization for composite materials is done for vertical static loading and the fatigue life control of composite structures was performed only with respect to these vertical forces. The fatigue life safety factor is checked for two different criteria as, Goodman criterion and the maximum strain in component.

2. Composites

One of the most important developments in the field of materials in the last century is composite materials. Composite materials are formed by the combination of at least two organic or inorganic components. One of the builders is the matrix, which is the main material, and the other is the fiber that serves as the load carrier. Fiber is a component that provides a great majority of the strength for the composite material. The matrix is holding fibers together to provide transferring of loads to fibers, protecting fibers against risks from external factors, providing resistance to crack growth and spreading, resists to high temperatures and corrosion.

Laminate composites are formed by stacking fiber-reinforced plies. After the stacking of the layers the temperature and pressure are applied through the press.

In Fig. 1, the micro and macro mechanical states of the composite materials can be seen in general terms. Fiber diameter, particle size and spacing between fibers and matrix are important parameters in terms of design. The interaction of all these elements with each other is examined with the micro mechanical model.

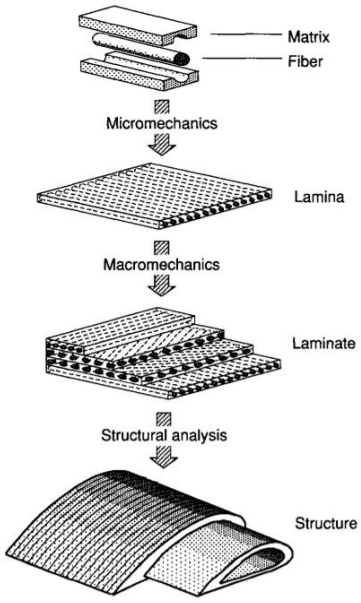

Fig. 1 Composite material structure (Daniel and Ishai 2006)

Laminates generally exhibit homogeneous properties but may also exhibit anisotropic behavior. For this reason, average mechanical properties are used at this stage during the analysis. The type of analysis carried out in this way is called macro mechanic analysis and the unidirectional laminate properties are used for semi-homogeneous anisotropic structure with average stiffness and strength. In laminate constructions, macro mechanical analysis is considered as the function of stacking of plies and the behavior of them. In this way the laminate theory is applied for composites. As a result, the finite element analysis is performed with the help of classical laminate theory.

3. Fatigue in composites

At first glance it can be said that composite material fatigue and metal fatigue are similar to each other. Both processes consist of crack initiation, crack propagation, and damage formation phases. The fatigue life for both materials, N_f fatigue life, is the sum of damage initiation N_i and damage progression N_p processes.

One of the differences is the relative durations for damage initiation and damage progression phases. In metals, the majority of the fatigue process is the progression of a single crack. The process in which the crack occurs is neglected in the metals due to micro-cracks already present in the metal such as dislocations. Crack progression is long due to hardening process. When the crack tries to advance, plasticity occurs at the crack tip, causing hardening. Crack hardening and crack propagation can be repeated over thousands of cycles. For this reason, it can be said that the fatigue life of metals is equal to the crack propagation life N_p.

Hardening of composite materials may be neglected. This is because of the crack progression time is much shorter than the crack initiation time for composites. Damage occurs very suddenly when a single crack nucleation occurs at a sufficient size. For this reason, the fatigue life N_f of the fiber-reinforced composites is considered equal to the crack initiation life N_i (Harris 1999, Talreja and Singh 2012).

Three principles are used for fatigue modeling of composite materials. These are S-N diagrams or Goodman diagrams, fatigue models using progressive failure models and calculating the residual mechanical properties of the material (Nijssen 2006, Talreja and Singh 2012).

Since fatigue behavior modeling with S-N curves is suggested for metal materials, this expression is insufficient for composite materials due to the inability of considering fully affect the properties of the composite constituents. Unless the effect of these components is determined precisely, many fatigue curves will emerge resulting in combinations of many factors such as fiber orientation, volume fiber ratio, layer sequence, geometric factors.

Concept fatigue life diagrams were introduced by Talreja and Singh (2012) to avoid this situation and to provide a basic model for the fatigue of composite materials. In this diagram, the horizontal axis represents the number of cycles as in the classical S-N curves, while the vertical axis represents the strain. In Fig. 2 the diagram shows the general structure for the composites under the periodic tensile load with the unidirectional fiber structure. Region 1, is the area in which the composite strain (ε_c) is expressed by fiber strain. Region 2 refers to the region intersecting the first region with low cycle numbers and reaching the fatigue limit (ε_m) asymptotically at high cycle numbers. Region 3 is below the fatigue limit. In this region, there is no damage for 10^6 cycles considered in most applications.

For glass fibers ε_c value is bigger than 2%, while for high-rigidity carbon fibers it is less than 0.5% (Talreja and Singh 2012).

The best way to examine the fatigue strength of laminates is through the test process. Number of tests and researches should be increased for the purpose of increasing the accuracy of the theories. Although fatigue models of composite structures are based on empirical statements, they are in a better position than metals in terms of fatigue performance.

When the applied force deviates from the fiber direction, the fiber-matrix interface is subjected to normal and shear stresses. These two combined stresses then cause interface cracks that can grow with cyclic loading. In case of larger loading angles than a few degrees, there is no longer a fiber damage that can divide the component into two. For this reason, region 1 no longer appears in the fatigue diagram, as shown in Fig. 3. As the loading angle increases, the 2nd region band

appears at lower strain levels and smaller slopes. The fatigue limit ε_m also drops due to the increased normal stresses at the interface caused by the increased loading angle. The lowest fatigue limit ε_{db} occurs when the loading angle is 90° which is perpendicular to the fibers. The dominant damage mechanism in this region is cross fiber separation (Talreja and Singh 2012).

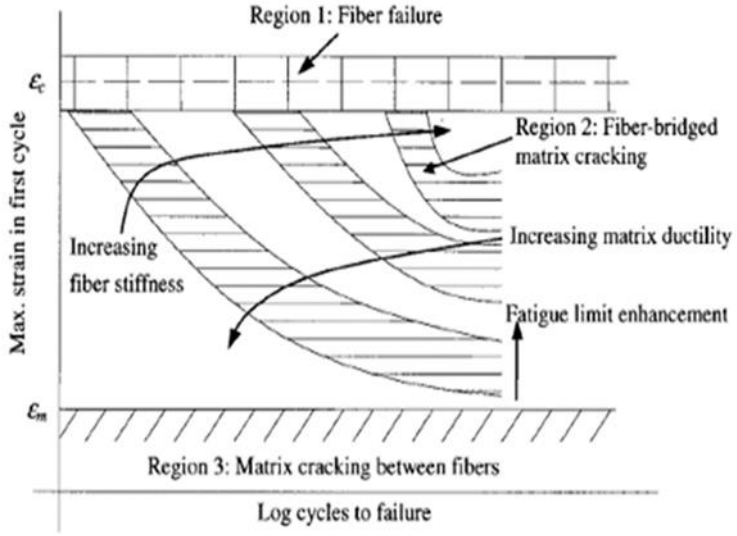

Fig. 2 Composite fatigue life diagram (Talreja and Singh 2012)

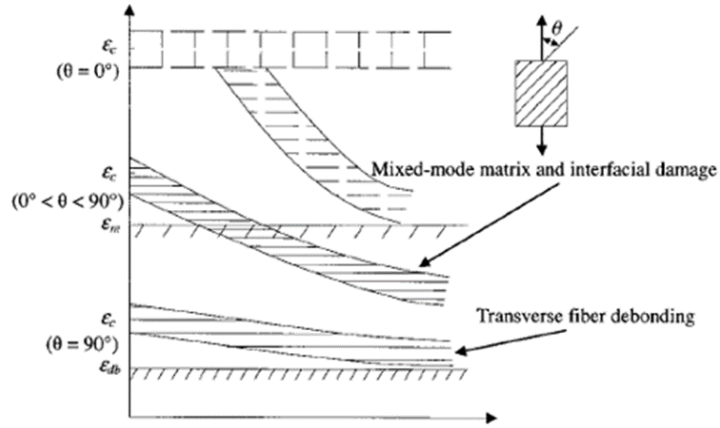

Fig. 3 Fatigue life of a unidirectional composite exposed to tensile load at certain angles to fiber direction (Talreja and Singh 2012)

4. Finite element model

The solid model has 4 axes. The longitudinal and transverse beams are welded in the original model. To facilitate solution in the finite element optimization, these welding connections are removed during geometrical cleaning and the transverse beams are connected directly to the

longitudinal beams, so monolithic structure has been obtained. The original model and dimensions can be seen in Figs. 4(a)-(b). The model is 9900 mm in length and 896 mm in width. The chassis is formed by combining U-profiles in various sizes.

The model is transferred from Solidworks environment to Hypermesh program. After that, by "Midsurface" operation, shell structure of chassis was obtained. Then finite element model is prepared as it can be seen from Figs. 5 and 6. The boundary conditions applied as encastre conditions on axle connection regions on chassis. The model consists total of 147.948 second order quad elements, the total node number is 449.44. For avoiding shear locking on shell elements fully integrated second order elements have been used.

According to Article 128 of the Turkish Highway Traffic Regulation (2015), the vehicle dimensions on the road were determined for cases loaded and unloaded, and also weights are determined that could be safely supported without damaging the road structure. The maximum weight of the truck was 32 tons, since the model have 4 axles. In the case of 32 tons weight, the front 2 axes carry 13 tons of weight and the remaining 19 tons are assumed to be transmitted by the rear two axes. The structure was divided into two groups and distributed loads were applied to that regions as front body part and rear body part.

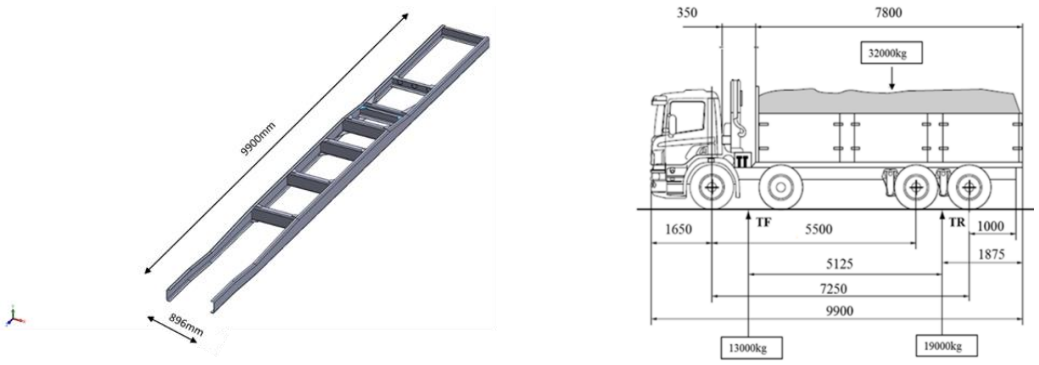

(a) Chassis CAD model (b) Truck dimensions

Fig. 4 Vehicle model

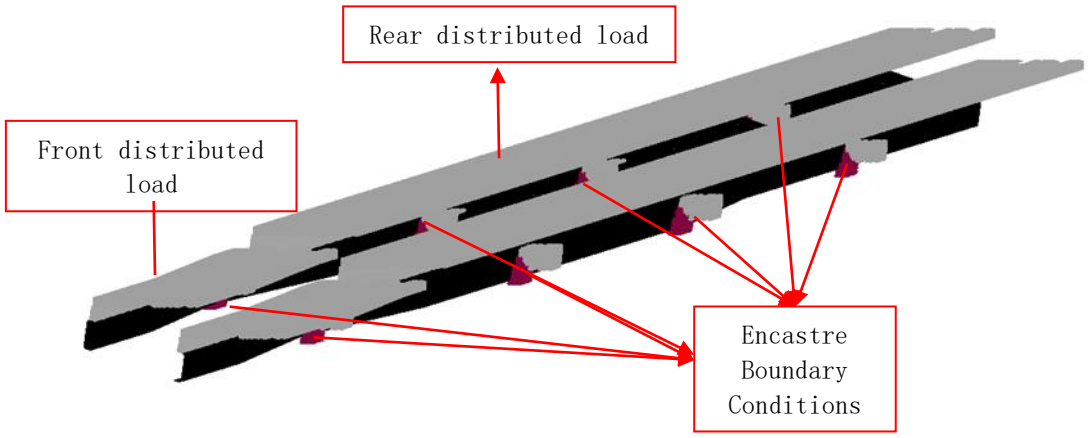

Fig. 5 Full scale finite element model of chassis with boundary conditions and loads

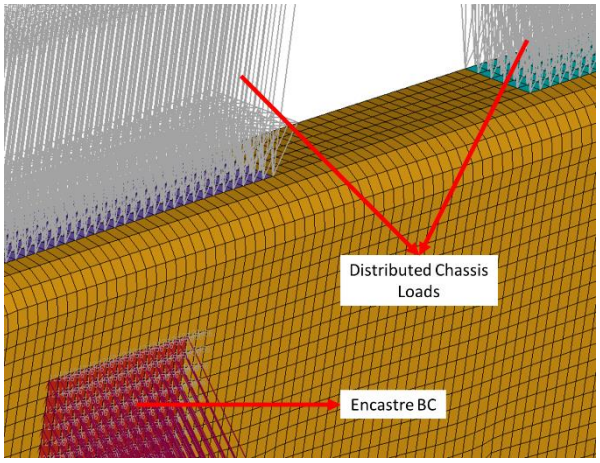

Fig. 6 Loads and boundary conditions on finite element model of chassis

4.1 Design spectra for dynamic case

It is a method in which dynamic forces are calculated and fatigue analysis can be performed under a specific "Design Spectra" prediction by taking advantage of the dynamic lateral load coefficient and the dynamic vertical force coefficient found by the help of tire data and wheel load. The dynamic forces calculated by this method can be applied both directly to the conventional design procedure and the computer based finite element model. Stress amplitudes can be controlled in terms of fatigue according to Goodman diagram (Yay and Ereke 2001).

In the first step, the tire outer diameter (D), the static radius of the tire (r_{st}), the maximum carrying capacity of the tire (N_{max}), the tire pressure (p_{max}) corresponding to (N_{max}), nominal load (N) and pressure corresponding to nominal load (p) are selected from tire catalog.

After that calculations are done by Eqs. (1)-(2)-(3)

Deflection (cm);

$$f = \frac{D}{2} - r_{st} \tag{1}$$

Tire spring coefficient at maximum capacity (kg/cm);

$$c_R = \frac{N_{max}}{f} \tag{2}$$

Tire spring coefficient at nominal load (kg/cm);

$$c_1 = \frac{p}{p_{max}} c_R \tag{3}$$

By using these calculated values and diagrams in Fig 7. the dynamic coefficients below are calculated (Yay and Ereke 2001),

k_1: Dynamic vertical force coefficient (Infinite life)

k_2: Dynamic vertical force coefficient (Finite life, Individual impact)

μ_{F1}: Dynamic horizantal force coefficient (Infinite life)

μ_{F2}: Dynamic horizantal force coefficient (Finite life, Individual impact)

The road conditions; which the vehicle will travel throughout its entire life; can be predicted as in Table 1.

The road distribution in Table 1 can be designed as desired by changing the ratios according to different operating conditions.

The forces for each road condition are given in Table 2. By taking into account the conditions described above, both the vertical dynamic force and the lateral dynamic force are calculated via Eqs. (4)-(5) which combines the life fractions forming the total life in Table 1 (Yay and Erek 2001). The two forces that are found are the forces that cover all road conditions in the design spectra. Therefore, the "DS" index is used to represent the "Design Spectra".

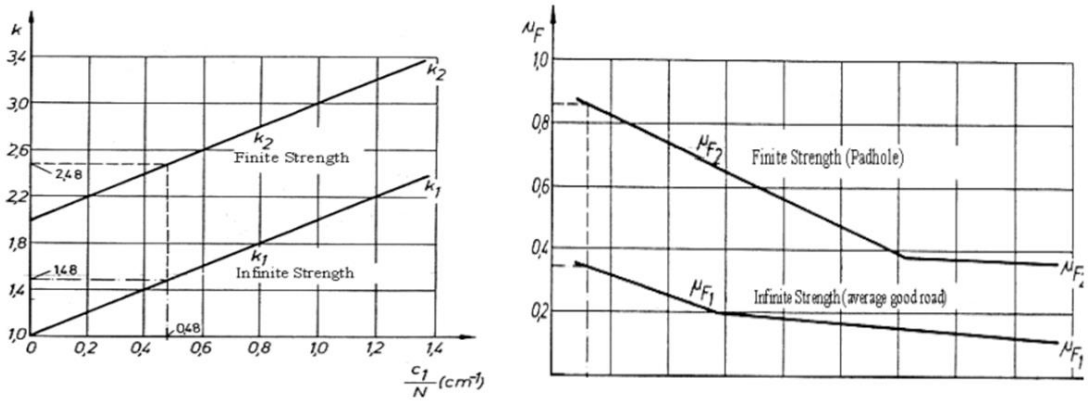

Fig. 7 Vertical and horizontal dynamic force coefficient diagrams (Yay and Ereke 2001)

Table 1 Road conditions of a vehicle throughout its entire life (Yay and Ereke 2001)

Road Type	Percentage of Total Life
Straight - Well Surface	n = 50
Straight - Bad Surface	$m_1 = 47$
Curved - Bad Surface	$m_2 = 2$
Individual Impact Surface	$m_3 = 1$

Table 2 Dynamic forces acting on the vehicle according to road conditions (Yay and Ereke 2001)

Road Type	Vertical Force	Horizontal Force
Straight - Well Surface	$P_{din\ well\ surface} = P_{static}$	-
Straight - Bad Surface	$P_{din\ bad\ surface} = k_1 \times P_{static}$	$S_{din\ bad\ surface} = \mu_{F1} \times P_{static}$
Curved - Bad Surface	$P_{din\ curved} = k_1 \times P_{static}$	$S_{din\ curved} = (0{,}25.\mu_{F1}) \times P_{static}$
Individual Impact Surface	$P_{din\ impact} = k_2 \times P_{static}$	$S_{din\ impact} = \mu_{F2} \times P_{static}$

$$P_{Din\ DS} = \left\{ \frac{Pdin\ bad\ surface}{100} m1 + \frac{Pdin\ curved}{100} m2 + \frac{Pdin\ impact}{100} m3 \right\} \left(1 + \frac{n}{50}\right) \quad (4)$$

$$S_{Din\ DS} = \left\{ \frac{Sdin\ bad\ surface}{100} m_1 + \frac{Sdin\ curved}{100} m_2 + \frac{Sdin\ impact}{100} m_3 \right\} \quad \left(1 + \frac{n}{50}\right) \quad (5)$$

Representation of the dynamic force graph which affects the wheel can be seen in Fig. 8.

The dynamic vertical force "$P_{Din\ DS}$", calculated as the force representing the design spectra, is the absolute value. By Eqs. (6)-(7) the amplitude value of force ΔP is calculated (Yay and Ereke 2001).

$$P_{Din\ DS} = P_{static} + \Delta P \tag{6}$$

$$\Delta P = P_{Din\ DS} - P_{static} \tag{7}$$

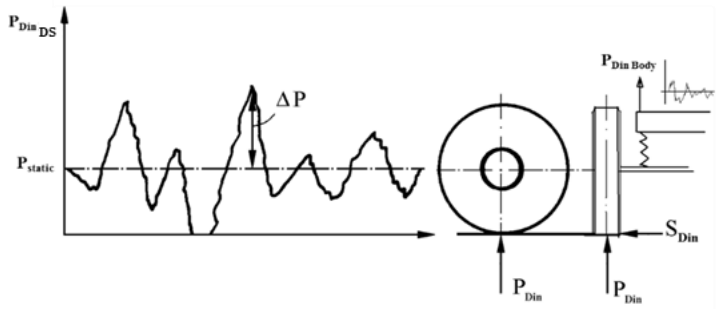

Fig. 8 The dynamic force amplitude representation graph acts on wheel

By using P_{static} value, mean stress value σ_m is found. ΔP value is also used to calculate the amplitude stress value σ_{amp}. After that equivalent stress is found by adding the stresses that will come from the lateral force itself in the horizontal plane. Fatigue control of the cross section is carried out with the Goodman diagram by using this equivalent stress value.

Analyses were made using the Optistruct solver. The chassis model in which the steel material is assigned is approximately 650 kg.

The tire type is selected as 1200 R 20, considering the axle loads to be met by the vehicle tires. In the case of a maximum load of 32 tons, the front axle takes the 13 tonnes of total weight and a 3500 kg load corresponds to per tire. The rear eight wheels takes the remaining 19 tonnes of load with a load of 2375 kg per tire. Tire datas such as static radius, diameter, maximum, nominal pressure values and maximum and nominal load values are taken from Hankook (2012) tire catalog, and dynamic force coefficients from the graphs in Figure 6 for each axle are calculated.

5. Finite element model with composite material and optimization

Structural optimization has become important to all industries over the last decade, recognizing the gains it has made in the conceptual design phase. Two-stage optimization for metal constructions has been used successfully. In the first stage, topology optimization is used to form the overall concept, while in the second stage, detailed design is created by sizing and shape optimization. Additional design variables for composite structures require modifications in the optimization process. Although composite materials can be formed in many different forms, their general use is to bring the thin plies stacked in different orientations and to form the shell structure. In recent years, a 3-phase optimization process has been developed for composite

materials (Zhou *et al*. 2009, 2011).

Optistruct solver is used to optimize the composite material on the chassis model. One of the biggest difference between steel material and composite materials is seen in the modulus of elasticity. The steel material performs better in terms of displacements due to its high modulus of elasticity. In order to eliminate this disadvantage of the composite material and provide appropriate design, it is aimed to maximize the structural rigidity as an objective function in the optimization study. By this way, proper and realistic design will be provided while weight reduction is achieved. Fig. 9 which was given by Zhou *et al.* (2011) shows the phase flow and general optimization operation.

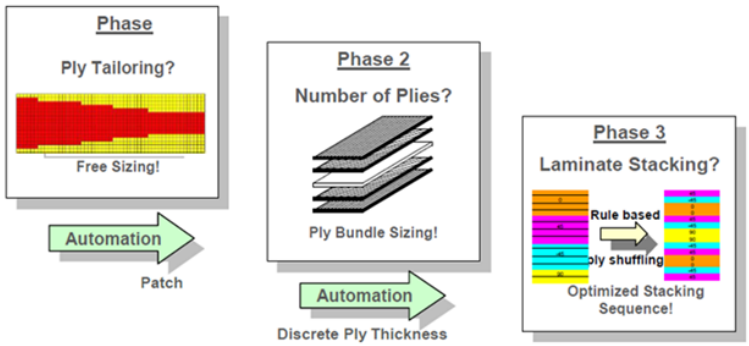

Fig. 9 Illustration of optimization phases (Zhou *et al.* 2011)

5.1 Optimization phases for composites

5.1.1 Phase-1: Free-size optimization

The aim of the first phase is to determine the material distribution within the structure in terms of orientation and thickness. In this process, it is ensured that the thicknesses of these plies can be changed freely by using the super-ply definition, each with its own fiber orientation. As a result, the thickness distribution of each fiber orientation is obtained throughout the structure (Zhou *et al*. 2009, 2011).

The super-ply definition is defined in the analysis as the purpose of providing the virtual thickness variation for each fiber orientation in any region of the composite material stack. Shell structures are used for planar loads as they also provide bending capacity, and typically a single super-ply definition is required for each fiber orientation. In the design phase, usually "compliance" or displacement reactions are used to optimize the total stiffness of the structure (Zhou *et al*. 2009, 2011).

5.1.2 Phase-2: Size optimization

At the end of phase-1, continuous thickness distribution is obtained for each fiber orientation. Here, the thicknesses of the plies in each orientation are given in total. Each thickness value specified separately is the sum of the plies in the same orientation. In this way, plies of different fiber orientations are placed together to form composite laminate. All the production constraints mentioned in phase 1 are carried to this stage (Zhou *et al*. 2009, 2011).

5.1.3 Phase-3: Ply bundle stacking optimization

At the end of phase-2, although the layout and stacking order is obtained for all bundles, production constraints are generally not achieved. Optimization is done to determine the position of each ply in the laminate to ensure that manufacturing constraints are satisfied with previous design constraints. Some of the key manufacturing constraints are (Zhou *et al.* 2009, 2011);

- Pairing of +/- orientations.
- Preset cover sequencing.
- Preset core sequencing.
- Limiting consecutive plies of the same orientation.

5.2 Finite element modeling for composite optimization

Four different fiber angles were used in the optimization as 0^0, 90^0, $+45^0$, -45^0. The four different super-plies described were put in a single laminate. The composite material is defined as orthotropic. The element normal and element orientations should be carefully checked for finite element analysis of composite structures. Differences in some element normals or differences in element orientations can lead to incorrect results in optimization (Altair Engineering 2012). For this reason, the element normals and material orientations are arranged as shown in Fig. 10. The element normal are set to towards outside (blue in figure). The fiber orientations were set so that the 0 degree fiber angle would follow the longitudinal direction of the beams.

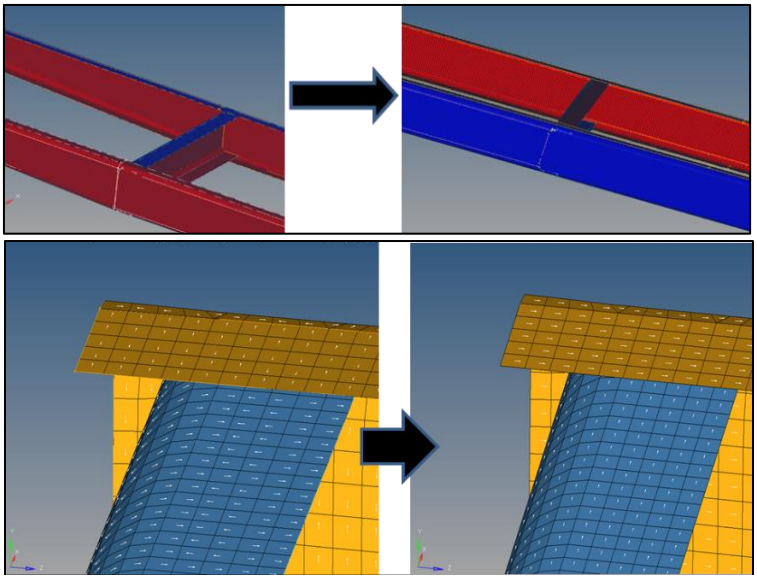

Fig. 10 Element normals and material orientations in finite element model

In phase-1, optimization design variable was defined first. The minimum and maximum thickness values that can be used for the laminate, the fiber orientations desired to be balanced with each other are defined in the design variant. Later on, four different response functions were defined as mass, vertical displacement, lateral displacement and compliance. The objective

function of the optimization is defined as minimizing the function of the compliance, in other words maximizing the rigidity. Furthermore, in order to keep the in-plane shear stresses in the composite material at a certain level, certain values were set according to Hoffman's theory.

While the maximum mass for the lightweight structure is limited to 350 kg, the vertical displacement is limited to 20 mm and the lateral displacement is limited to 15 mm at the body end region for proper service and conformt.

After completion of phase-1, all boundary conditions, reaction functions and objective function defined earlier are carried to phase-2. The ply thicknesses obtained at the end of phase-1 are not realistic and cannot be produced. For this phase, 16 automatic layers were created by the program at 4 angles given in phase-1. For each of these layers, size optimization is achieved by giving minimum and maximum ply thicknesses again. In addition, for each layer, the producible ply thickness values are given to obtain the total number of layers required for each angle.

Optimum layer alignment was achieved in phase-3. Here, pair formation is provided with the + 45^0 and -45^0 fiber orientations to avoid creating extra torsion in the structure.

The mechanical properties of unidirectional continuous composite materials AS4-PEEK and EGlass-epoxy can be seen in Table 3. The modulus of elasticity in the fiber direction is E11, the modulus of elasticity in the transverse direction is E22, the G12 is shear modulus, the μ12 is poisson ratio, tensile strength in the fiber direction is F1t, the compressive strength in the fiber direction is F1c, the tensile strength in the transverse direction is F2t, the compressive strength in the transverse direction is F2c and F6 indicates the shear strength (Hexcel 2014).

Table 3 Mechanical properties of composite materials (Hexcel 2014)

Composite Materials Mechanical Properties	AS4-PEEK	Eglass-epoxy
Fiber	AS4 Carbon	Glass fiber
Matrix	APC2 PEEK	Epoxy
Vf	0,58	0,55
ρ (g/cm^3)	1,57	2,1
E11(Gpa)	131	39
E22(Gpa)	8,7	8,6
G12(Gpa)	5	3,8
μ12	0,28	0,28
F1t(MPa)	2060	1080
F1c(MPa)	1080	620
F2t(MPa)	78	39
F2c(MPa)	196	128
F6(MPa)	157	89

In the optimization process with AS4-PEEK material, the super-layer thicknesses at 4 different angles defined in Phase-1 were initially taken as 8 mm. The reason for the large thickness is that the optimization algorithm does not add any material after initial definition, but instead the material is removed step by step.

Optimization constraint is defined as the maximum shear stress between layers for AS4-PEEK is to be below 100 MPa according to Hoffman's theory.

For the design variable function, the minimum thickness of the laminate structure is limited to 4 mm and the maximum thickness is limited to 24 mm. In order to avoid extra torsion in the structure, balancing of layers in fiber orientations of +45 and -45 is added as a constraint.

In Phase-2, in addition to the design variable defined in Phase-1, 16 automatic layer variables are created. The design interval was defined by giving the manufacturable thickness ranges for each of these 16 variables as inputs to the program. At this stage, the thickness of the manufacturable layer for AS4-PEEK was determined to be 0.2 mm.

At the end of Phase-3, 121 layers emerged. The 121 layers that emerged at the end of Phase-2 are arranged in the order they are described. The stackup sequence of these plies was carried out in Phase-3. At this stage it is defined that the layers with +45 and -45 fiber orientations should form pairs.

EGlass-epoxy has lower mechanical properties than AS4-PEEK material. In the optimization process with EGlass-epoxy material, the super-layer thicknesses at 4 different angles defined in Phase-1 were initially taken as 9 mm.

Optimization constraint is defined as the maximum shear stress between layers for EGlass-epoxy is to be below 50 MPa according to Hoffman's theory.

For the design variable function, the minimum thickness of the laminate structure is limited to 4mm and the maximum thickness is limited to 32 mm. In order to avoid extra torsion in the structure, balancing of layers in fiber orientations of +45 and -45 is added as a constraint.

At Phase-2 the thickness of the manufacturable layer for EGlass-epoxy was determined to be 0.2 mm.

At the end of Phase-3, 153 layers emerged. The 153 layers that emerged at the end of Phase-2 are arranged in the order they are described. The stackup sequence of these plies was carried out in Phase-3. At this stage it is defined that the layers with +45 and -45 fiber orientations should form pairs.

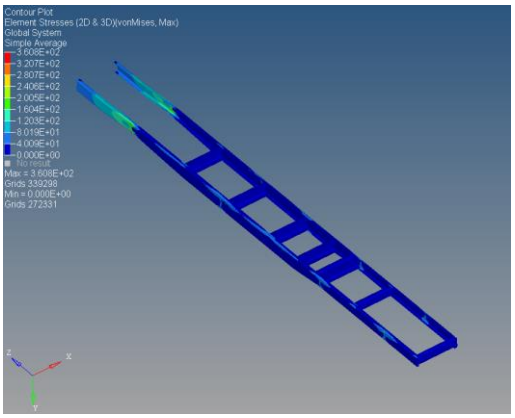

Fig. 11 Von Mises stress contour of steel chassis for static loading

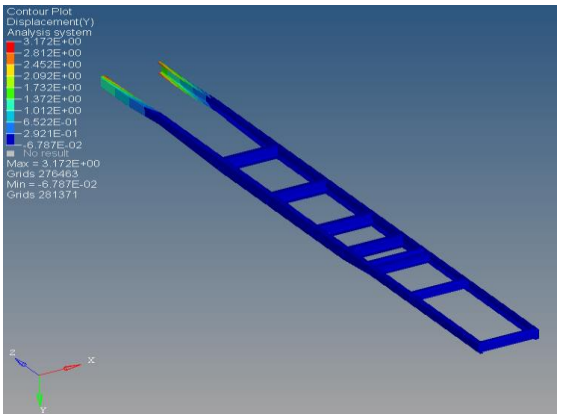

Fig. 12 Von Mises stress contour of steel chassis for dynamic loading

6. Analyzes results

6.1 Steel material results

The chassis material was taken as St-52 steel, with a tensile strength of 520 MPa. The fatigue strength of material is taken as 40% of the tensile strength.

When these values are checked according to the Goodman curve by Eq. (8), the safety factor is S = 2.74, which means the body has infinite life in terms of fatigue.

In the calculations, the stresses were taken according to von Misses and the notch coefficient was taken as $K_f = 1.5$.

$$\frac{K_f s_g}{s_{D*}} + \frac{\sigma m}{\sigma tensile} = \frac{1}{S} \tag{8}$$

The Von Mises stress contour on steel chassis can be seen for static and dynamic loadings in Figs. 11 and 12, respectively.

6.2 Composite materials results

6.2.1 Optimization results

AS4-PEEK

At the end of phase-2, the total thickness of the laminate was 22 mm in majority of the structure for given requirements and constraints. This can be seen in Fig. 13.

The 121 ply for profiles at the end of phase-2 can be seen in Fig 14. At the end of phase-2, the total chassis weight is approximately 326 kg.

The composite material damage index at the end of phase-3 can be seen in Fig. 15. The maximum composite damage index is 0.41 which is well below 1.

At phase-3 material removal is not performed. The arrangement of the plies, given at the end of phase-2, is optimized according to the requirements.

At the end of phase-3, the performance of the structure was again evaluated according to displacement, stress and damage indices. The maximum vertical displacement is approximately 15.6 mm below the target value. The maximum lateral displacement is 11.3 mm which is also below target value.

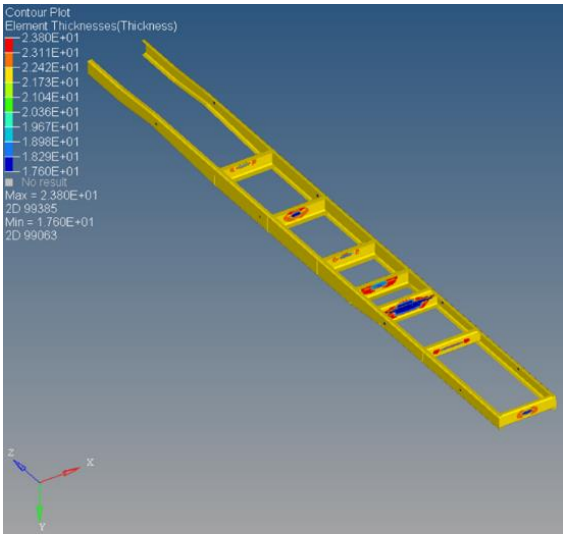

Fig. 13 Total laminate thickness distribution at the end of phase-2 for AS4-PEEK composite material

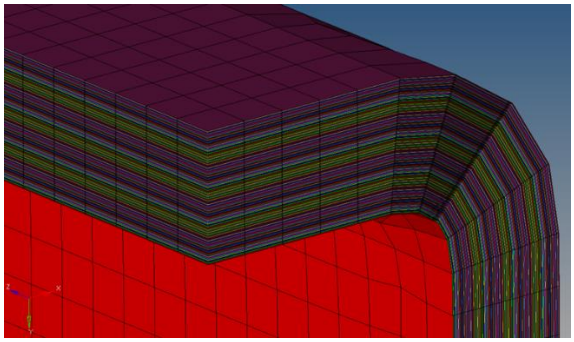

Fig. 14 121 layers formed at the end of Phase-2

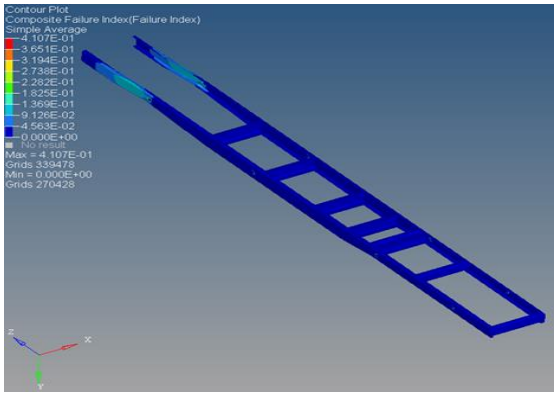

Fig. 15 AS4-PEEK composite damage index

EGlass-epoxy

The maximum total laminate thickness at the end of phase-2 in the direction of given requirement and constraints is decreased to 31 mm from 36 mm in longitudinal beams. This can be seen in Fig. 16.

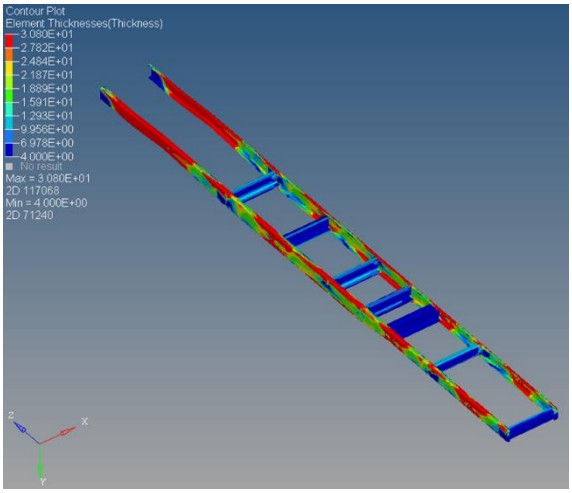

Fig. 16 Total laminate thickness distribution at the end of phase-2 for EGlass-epoxy composite material

The 153 plies formed at the end of phase-2 can be seen in Fig. 17. At the end of phase-2, the total chassis weight is approximately 345.5 kg.

At the end of phase-3, the performance of the structure was again evaluated according to displacement, stress and damage indices. The maximum vertical displacement is approximately 18.7 mm below the target value. The maximum lateral displacement is also below the desired level with 6.5 mm.

The composite material damage index at the end of phase-3 can be seen in Fig. 18. The maximum composite damage index is 0.64 which is below 1.

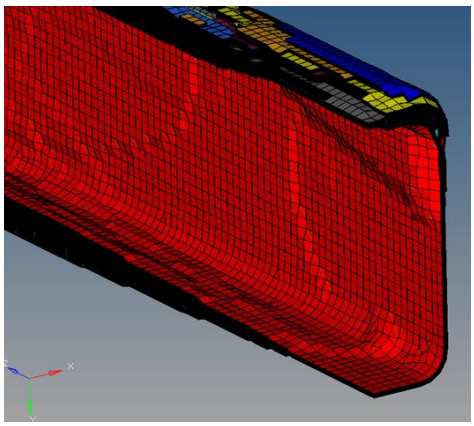

Fig. 17 153 layers formed at the end of Phase-2

6.2.1 Fatigue control for optimized composites

The fatigue control of the composite materials was first performed using the modified Goodman-Boller fatigue model for composite materials. For both composite materials, the S-N curve data obtained from the loading condition R = 0.1 tests in the literature were used and the fatigue life was checked according to this loading condition (Mandell and Samborsky 1997, 2002, Talreja and Singh 2012). Secondary fatigue control was carried out by checking the maximum amount of strain in the composite material and checking whether these values exceed the minimum amount of strain that could lead to the crack initiation in the matrix.

According to the Goodman-Boller criterion, the fatigue control is made for both the fiber direction and transverse direction. The stress concentration factor is taken as 3 for the bending state.

The minimum fatigue strain for PEEK material was set as 0.5%. It is predicted that the matrix crack formation will not start with the safety factor of S = 1.56 and the material will work safely for 10^6 cycles, even the maximum strain is 0.3189% in the maximum load for the static state on the AS4-PEEK composite structure.

The minimum fatigue strain for epoxy material was set as 0.46%. It is predicted that the matrix crack formation will not start with the safety factor of S = 1.24 and the material will work safely for 10^6 cycles, even the maximum strain is 0.3702% in the maximum load for the static state on the Eglass-epoxy composite structure.

Table 4 shows the fatigue safety coefficients of the fatigue controls for the optimized composite structure.

Table 4 Fatigue safety coefficients of the optimized composite structure

	Goodman-Boller - Safety Coefficient	Maximum Strain - Safety Coefficient
AS4-PEEK Fiber Direction	21.3	1.56
AS4-PEEK Transverse Fiber Direction	9.55	1.56
EGlass-Epoxy Fiber Direction	14.58	1.24
EGlass-Epoxy Transverse Fiber Direction	1.63	1.24

7. Conclusions

The outputs obtained from the finite element analysis can be seen for steel, AS4-PEEK and EGlass-epoxy materials in Table 5.

Table 5 Dynamic forces acting on the vehicle according to road conditions

	Steel	AS4-PEEK	Eglass-Epoxy
Maximum Vertical Displacement(mm)	11.8	15.6	18.7
Minimum Fatigue Life (Cycle)	10^6	10^6	10^6
Total Weight (kg)	650	326	345.5
Weight Reduction (%)	-	49.8	46.8

As it can be seen from the Table 5, using composite material instead of steel provides a weight reduction of up to 50%. In order to obtain close performance values as steel, in the optimization made with AS4-PEEK material, much material has been used. By allowing a little more displacement values, 326 kg weight can be reduced to 300-250 kg range. Although the displacement values are close to the limit values with the EGlass-epoxy composite material, the weight reduction provided by the carbon fiber is almost achieved. From these results it has been understood that more detailed designs with composite structures can result in substantial weight reductions in the vehicle chassis.

Composite materials have high durability and high fatigue strength and have the potential to be competitive in conventional steel. Increased displacements due to relatively low modulus of elasticity of composite materials is a problem that can be overcome by design optimizations. In this way, weight reduction can be improved by up to 50%, and significant reductions in fuel consumption and exhaust emissions can be achieved.

Composite fatigue, which is the subject of the study, is a research area that requires serious study. In composite structures, the use of conventional S-N curves for metals can lead to incorrect results. In the first phase of the study, it was aimed to apply conventional Goodman fatigue diagrams for composite materials, but in the direction of research conducted, it was found that the use of the Goodman fatigue model for composites depends on the empirical statements to be correlated with many experiments. Because the study was carried out with analyzes based on the application of the Goodman fatigue model, the fatigue control of the composite materials was first performed using the modified Goodman-Boller fatigue model. For both composite materials, the S-N curve data obtained from the loading condition R = 0.1 tests in the literature were used and the fatigue life was checked according to this loading condition. The reason for the fatigue safety coefficients, which are relatively low according to the strain control, is that the possibility of crack initiation is taken into account in this control. All these controls are preliminary controls for the concept design that is optimized. Detailed designs should be carried out with more detailed and verified tests.

For more detailed analysis of composite materials, progressive damage models and detailed finite element models and micromechanical analyzes should be used. Composite fatigue is seriously affected by many factors such as fiber orientation, ply thicknesses, layer sequencing,

fiber ductility, matrix ductility, loading angle. For this reason, the theoretical calculations and analyses made in the individual of each design must be tested and the correlated.

Note

This paper is revised and expanded version of a paper entitled "Composite material optimization for heavy duty chassis by finite element analysis" presented at OTEKON2016, 8. Automotive Technologies Congress, Bursa, 23-24 May, 2016.

References

Altair Engineering GmbH (2012), *Practical Aspects of Structural Optimization*, Altair Engineering GmbH, California, U.S.A.

Altair Engineering GmbH (2012), *RADIOSS/OptiStruct Reference Guide V11.0*, Altair Engineering GmbH, California, U.S.A.

Altair Product Design.

Article 128 of the Turkish Highway Traffic Regulation (2015), *Karayolları Trafik Yönetmeliğinde Değişiklik Yapılmasına Dair Yönetmelik*, Karayolları Genel Müdürlüğü, Ankara, Turkey.

Campbell, F.C. (2010), *Structural Composite Materials, Introduction to Composite Materials*, ASM International, Ohio, U.S.A.

Daniel, I.M. and Ishai, O. (2006), *Engineering Mechanics of Composite Materials*, Oxford University Press, New York, U.S.A.

Hankook Tire Company (2012), *Hankook Tire Truck & Bus Tyre Technical Manual*, Hankook Tire Europe, Neu-Isenburg, Germany.

Harris, B. (1999), *Engineering Composite Materials*, The Institute of Materials, London, U.K.

Hexcel (2014), *HexForce Reinforcements: Technical Fabrics Handbook*, Stamford, Connecticut, U.S.A.

Knouff, B., Batten, J., Eberle, C. and Eberhardt, J. (2006), *Advanced Composite Support Structures*, FY 2006 Progress Report for High Strength Weight Reduction Materials, Office of FreedomCAR and Vehicle Technologies, U.S. Department of Energy, Washington, U.S.A., 115-118.

Lavender, C.A., Knop, K.M. and Eberhardt, J.J. (2006), *New-Generation Frame for Pickup/Sport Utility Vehicle Application*, FY 2006 Progress Report for High Strength Weight Reduction Materials, Office of FreedomCAR and Vehicle Technologies, U.S. Department of Energy, Washington, U.S.A., 119-121

Mandell, J.F. and Samborsky, D.D. (1997), *DOE/MSU Composite Material Fatigue Database: Test methods, Materials, and Analysis*, Research Report No. SAND97-3002, Sandia National Laboratories, Albuquerque, NM.

Mandell, J.F., Samborsky, D.D. and Cairns, D.S. (2002), *Fatigue of Composite Materials and Substructures for Wind Turbine Blade*, Contractor Report No. SAND2002-077, Sandia National Laboratories, Albuquerque.

Nijssen, R.P.L. (2006), *Fatigue Life Prediction and Strength Degradation of Wind Turbine Rotor Blade Composites*, Research Report No. SAND2006-7810P, Sandia National Laboratories, Albuquerque.

Talreja, R. and Singh, C.V. (2012), *Damage and Failure of Composite Materials*, University Press Cambridge, Cambridge, U.K.

Tsai, S.W. (1996), *Strength Characteristics of Composite Materials*, Contractor Report No. NASA CR-224, National Aeronautics and Space Administration, California, U.S.A.

US Department of Energy (2013), *Workshop Report Trucks and Heavy-Duty Vehicles Technical Requirements and Gaps for Lightweight and Propulsion Materials*, US Department of Energy, U.S.A.

Yay, K. and Ereke, İ.M. (2001), *Fatigue Strength of a Rim Model with FEM Using a New Approximation*

Technique, Automotive and Transportation Technology Congress and Exhibition, SAE, October, Barcelona.

Zhou, M., Fleury, R. and Dias W. (2009), "Composite design optimization-from concept to ply-book details", *Proceedings of the 8th World Congress on Structural and Multidisciplinary Optimization*, Lisbon, Portugal, June.

Zhou, M., Fleury, R. and Kemp, M. (2011), *23. Optimization of Composite: Recent Advances and Application*.

FO